Synthesis and Tissue Distribution of (*m*-[^{125}I]Iodobenzyl)trozamicol ([^{125}I]MIBT): Potential Radioligand for Mapping Central Cholinergic Innervation

S. M. N. Efange,*,†,‡ R. H. Michelson,† A. B. Khare,† and J. R. Thomas†

Departments of Radiology and Medicinal Chemistry, University of Minnesota, Minneapolis, Minnesota 55455

Received February 5, 1993

Racemic (*m*-iodobenzyl)trozamicol (**6**, MIBT), a high-affinity vesamicol receptor ligand, was radiolabeled, resolved, and evaluated in rats. Following iv injection, (+)- and (−)-[^{125}I]MIBT achieved initial brain levels of 0.57 and 0.92% dose/g of tissue, respectively. The level of (+)-[^{125}I]MIBT subsequently declined by 74% within 3 h, while that of (−)-[^{125}I]MIBT remained stable for the duration. Ex vivo autoradiographic mapping of (−)-[^{125}I]MIBT distribution in rat brain revealed a pattern which was inconsistent with central cholinergic innervation. However, high levels of (+)-[^{125}I]MIBT were observed over the amygdala, striatum, nucleus accumbens, olfactory tubercle, and nuclei of the fifth and seventh cranial nerves, while moderate to low levels were detected within the cortex, hippocampus, and cerebellum. Thus, the distribution of (+)-[^{125}I]MIBT parallels that of other presynaptic cholinergic markers. Co-injection of (+)-[^{125}I]MIBT with 4-aminobenzovesamicol (**2b**), a potent vesamicol receptor ligand, reduced the levels of radiotracer in the striatum, cortex, and cerebellum by 58, 35, and 9%, respectively. Thus, (+)-[^{125}I]MIBT binds to vesamicol receptors in vivo. In contrast, coadministration of (+)-[^{125}I]MIBT with haloperidol (0.5 μmol/kg), reduced radiotracer levels in the cortex and cerebellum by 34 and 59%, respectively, while increasing the levels in the striatum by 32%. We conclude that although the distribution of (+)-[^{125}I]MIBT qualitatively reflects cholinergic innervation, a fraction of radiotracer in the cortex and cerebellum is bound to σ receptors.

Introduction

The discovery of the vesamicol receptor,[1,2] a cytoplasmically oriented site associated with the vesicular acetylcholine transporter, has provided a novel and potentially useful site for the study of presynaptic cholinergic function with radiotracer techniques. However, the prototypical vesamicol receptor ligand, 2-(4-phenylpiperidino)cyclohexanol (**1**, vesamicol), also exhibits significant α-adrenoceptor activity.[3,4] This limitation has provided the impetus for the development of more selective vesamicol receptor ligands. In an earlier study,[5] Rogers et al. identified the analogues **2–4** as potent ligands for this receptor. Subsequent studies[6] have demonstrated that 4-aminobenzovesamicol (**2b**) is a potent pseudoirreversible ligand for the vesamicol receptor, suggesting that the fused bicyclic fragment imparts to this molecule a high degree of complementarity for the receptor. Derivatization of the benzovesamicol nucleus, **2a**, has yielded potentially useful radiotracers for single photon emission computed tomography (SPECT) and positron emission tomography (PET).[7-12] However, only one attempt[13] has been made to utilize **4** as a prototype for radioligand development. The apparent preference for **2a** over **4** may be attributed to at least two factors: (a) the former is easily derivatized via **2b**, and (b) **2a** contains fewer stereogenic centers than **4**. Given the relative stereochemical simplicity of **2a**, the synthesis of its derivatives would involve fewer chiral resolution steps. The latter notwithstanding, the potency of **4** strongly suggests the following: (a) that the fused bicyclic system is not essential for high affinity and (b) that potent vesamicol receptor ligands may be obtained by single-point modification of the cyclohexyl moiety of the parent structure, **1**. In our search for a new class of vesamicol analogs which are amenable to facile functionalization, we have effected such a single-point modification to yield 4-azavesamicol (**5**, trozamicol).[14] Several *N*-arylakyl analogues of **5**, including **6** and **7**, are potent inhibitors of [^{3}H]ACh transport into cholinergic synaptic vesicles.[14] This paper describes the synthesis and biological evaluation of radiolabeled (*m*-iodobenzyl)trozamicol ([^{125}I]-**6**, [^{125}I]MIBT), one member of this novel class of vesamicol receptor ligands.

Chart I. Vesamicol and Derivatives

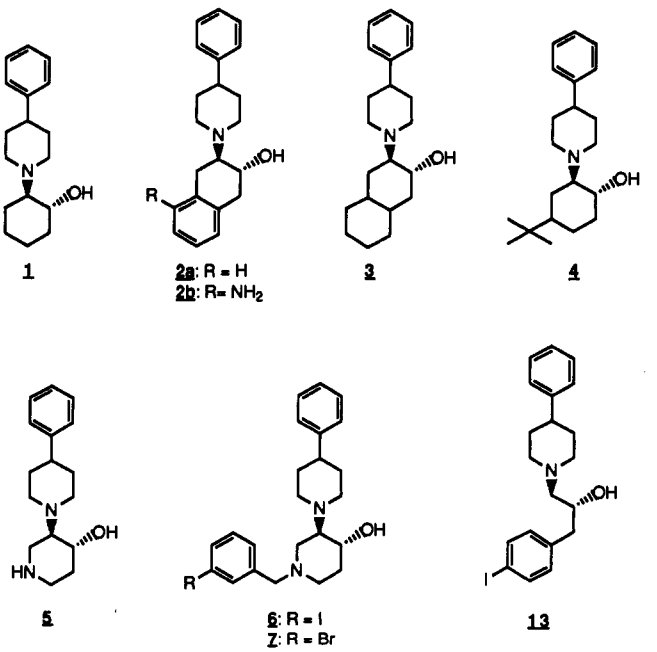

* Send inquiries to: S. Mbua Ngale Efange, Ph.D., Department of Radiology, Box 382 UMHC, University of Minnesota Hospital and Clinic, Minneapolis, MN 55455.
† Department of Radiology.
‡ Department of Medicinal Chemistry.

0022-2623/93/1836-1754$04.00/0

Scheme I. Synthesis of [^{125}I]MIBT (Method A)[a]

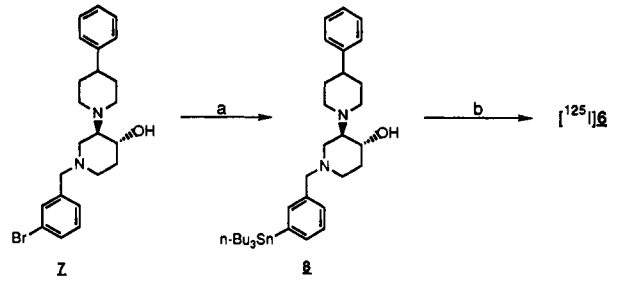

[a] (a) *n*-BuLi, *n*-Bu_3SnCl, −78 °C; (b) Na^{125}I(aq), Chloramine T, HOAc.

Scheme II. Synthesis of [^{125}I]MIBT (Method B)[a]

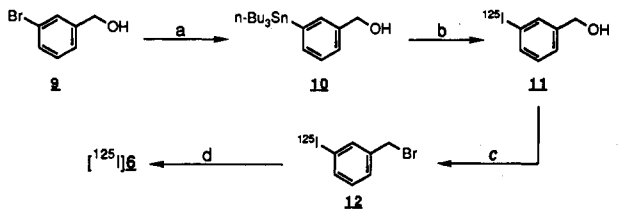

[a] (a) *n*-BuLi, *n*-Bu_3SnCl, −78 °C; (b) Na^{125}I, Chloramine T, HOAc; (c) 48% HBr, 90 °C; (d) (+)-5, DMF, Et_3N, 110 °C.

Chemistry

The synthesis of 4–7 has been reported.[14] Racemic 6 was resolved chromatographically on a Chiralcel OD column to yield (+)- and (−)-6 in greater than 99% ee. The tributylstannyl derivative 8 was obtained in 27% yield from 7 via a halogen–metal exchange–alkylation sequence (Scheme I).

Radiolabeling of 8 by oxidative iododestannylation proved problematic. The use of oxidants such as *N*-chlorosuccinimide and H_2O_2 in acidic media failed to yield the desired products. However, complex mixtures of unknown products were detected in the radiochromatogram. Similar results were obtained when Chloramine T was used as the oxidant in MeOH, in phosphate buffer (pH 7.8), and in NH_4OAc buffer (pH 4.2).

Finally, the use of Chloramine T in glacial HOAc yielded 42% of radiolabeled MIBT. However, several species accounting for up to 40% of the extractable radioactivity were visible in the radiochromatogram. Given the ease with which iododestannylation occurs in other aromatic or unsaturated systems,[9,15,16] we attribute these results to the presence of a benzylic amine. This functionality may be particularly sensitive to oxidation and thereby contribute to side reactions.

To circumvent these difficulties, the synthesis of radiolabeled MIBT was accomplished by an indirect method (Scheme II). Oxidative iododestannylation of **10** proceeded cleanly to yield *m*-[^{125}I]iodobenzyl alcohol, **11**. The latter was converted to *m*-[^{125}I]iodobenzyl bromide, **12**, which was reacted with (+)-**5** to yield the desired (+)-[^{125}I]MIBT. Although this sequence is longer than the earlier one, all the reactions proceed cleanly and in high yields. At the end of the sequence, crude (+)-[^{125}I]MIBT was generally obtained in 75–85% overall yield with radiochemical purities ranging from 87 to 93%. This method is therefore superior to the one discussed above. The purified product was stable (HPLC) at 4 °C for at least 4 weeks.

Results and Discussion

Biodistribution Studies. The results of the biodistribution studies are summarized in Table I. For (+)-[^{125}I]MIBT, 1.06% of the injected dose of radioactivity was detected in the brain at 5 min. This level declined by 73% over the course of the study. Similarly, the initial level of 1.0% in the heart declined by 90% over 3 h. In general, the levels of radioactivity for most tissues were found to decrease with time. However, the levels in the thyroid increased significantly, suggesting in vivo deiodination.

Following the iv injection of (−)-[^{125}I]MIBT, 1.67% of the radioactivity was found in the brain after 5 min. In contrast to the dextrorotatory antipode, the level of radioactivity in the brain remained relatively stable for the duration of the study. In the heart, the initial level of 0.99% decreased to 0.36% after 3 h. As seen earlier with (−)-[^{125}I]MIBT, high levels of radioactivity were found

Table I. Tissue Distribution of (+)- and (−)-[^{125}I]MIBT in the Rat

	% dose/g of tissue (range)			
tissue	5 min (n = 3)	30 min (n = 3)	60 min (n = 3)	180 min (n = 3)
	(+)-[^{125}I]MIBT			
blood	0.24	0.12	0.09	0.07
	0.23–0.26	0.10–0.13	0.08–0.10	0.05–0.07
liver	1.60	2.18	1.91	1.18
	1.30–1.80	2.03–2.28	1.63–2.07	1.12–1.24
lung	3.67	1.21	0.82	0.39
	2.96–4.26	1.06–1.34	0.60–1.15	0.35–0.42
kidney	2.25	1.32	0.87	0.50
	2.00–2.52	1.14–1.41	0.78–1.01	0.45–0.52
muscle	0.34	0.16	0.11	0.08
	0.24–0.46	0.15–0.18	0.10–0.13	0.06–0.11
spleen	0.76	1.07	0.86	0.44
	0.54–1.01	0.87–1.23	0.73–0.96	0.42–0.47
heart	1.14	0.26	0.15	0.10
	0.97–1.26	0.24–0.29	0.09–0.19	0.09–0.11
brain	0.57	0.36	0.27	0.15
	0.50–0.67	0.34–0.38	0.22–0.32	0.14–0.16
gonads	0.13	0.15	0.17	0.16
	0.12–0.15	0.13–0.16	0.15–0.19	0.16–0.17
thyroid	1.60	2.33	4.59	13.13
	1.26–1.89	1.87–3.09	3.65–5.81	11.81–15.60
		Ratios		
brain/blood	2.33	3.18	3.08	2.35
	2.16–2.67	2.77–3.61	2.62–3.47	2.06–2.83
heart/blood	4.68	2.33	1.70	1.60
	4.24–5.01	2.04–2.54	0.98–2.21	1.34–2.04
	(−)-[^{125}I]MIBT			
blood	0.22	0.11	0.10	0.10
	0.19–0.25	0.10–0.13	0.09–0.10	0.08–0.12
liver	2.07	2.35	2.63	2.23
	1.81–2.49	2.14–2.51	2.28–3.11	2.07–2.34
lung	5.90	3.21	2.41	2.01
	4.65–7.87	2.87–3.55	1.99–2.89	1.87–2.43
kidney	3.71	3.53	3.13	3.27
	3.23–4.07	3.29–4.10	2.62–3.52	3.02–3.66
muscle	0.46	0.30	0.28	0.27
	0.24–0.69	0.23–0.37	0.26–0.29	0.21–0.37
spleen	1.04	1.24	1.17	1.28
	0.92–1.10	1.20–1.30	1.00–1.37	1.25–1.31
heart	1.32	0.75	0.58	0.50
	1.14–1.50	0.72–0.77	0.55–0.64	0.48–0.52
brain	0.92	0.99	0.83	0.92
	0.83–1.07	0.91–1.10	0.74–0.95	0.86–1.01
gonads	0.19	0.23	0.17	0.20
	0.18–0.22	0.16–0.30	0.16–0.18	0.19–0.22
thyroid	2.67	3.15	5.87	11.55
	2.35–2.97	2.77–3.81	4.53–7.42	8.13–14.65
		Ratios		
brain/blood	4.27	9.06	8.51	9.87
	3.42–5.44	8.63–9.38	7.94–9.60	7.97–12.82
heart/blood	6.07	6.87	5.97	5.32
	5.43–6.71	6.04–7.34	5.40–6.48	4.75–6.37

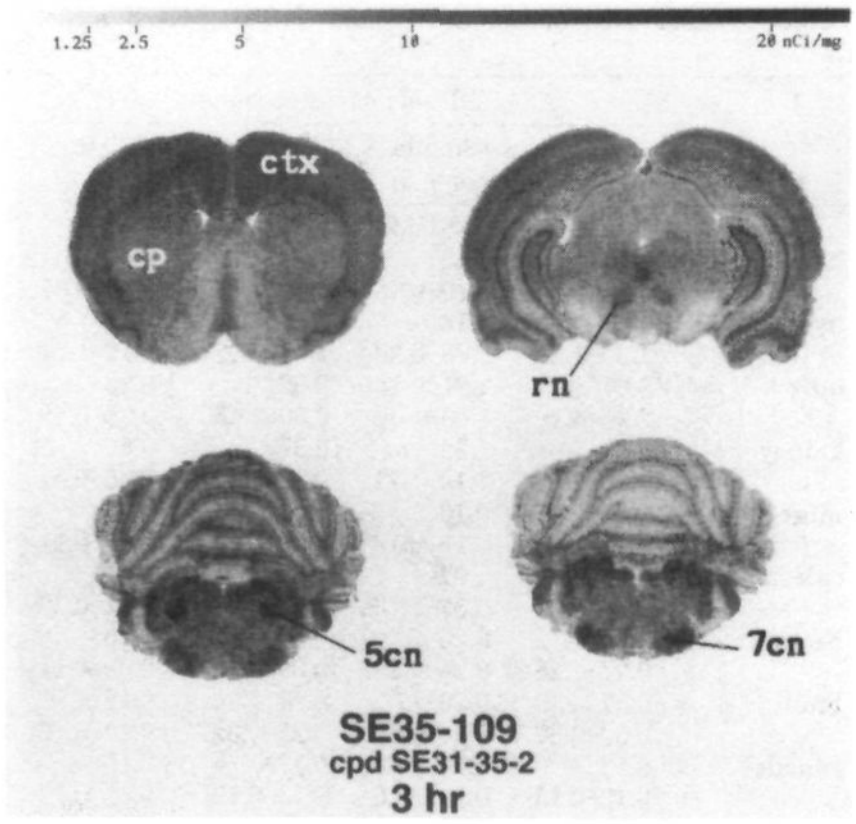

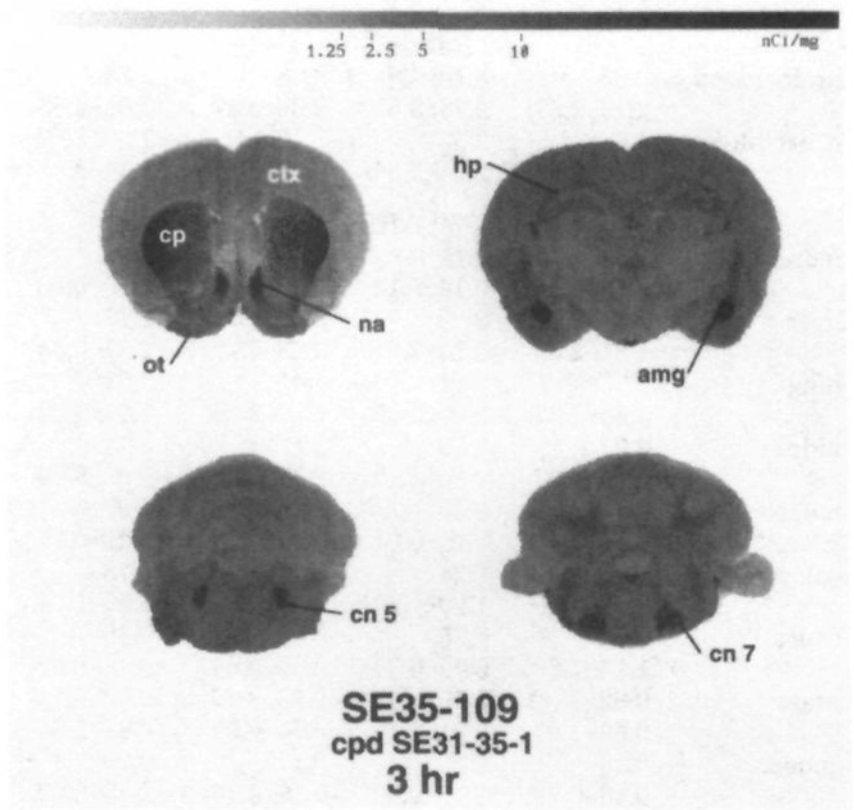

Figure 1. (a) Distribution of (−)-[^{125}I]MIBT in the rat brain as *revealed by autoradiography. (b) Distribution of* (+)-[^{125}I]*MIBT* in the rat brain as revealed by autoradiography. Legend: amg, amygdala; cp, caudate-putamen; ctx, cerebral cortex; cn, cranial nerve; hp, hippocampus; na, nucleus accumbens; ot, olfactory tubercle; rn, red nucleus.

within the thyroid following the administration of (+)-[^{125}I]MIBT.

Ex Vivo Autoradiography. The central distribution of (+)- and (−)-[^{125}I]MIBT as revealed by autoradiography is shown in Figure 1a,b. The levorotatory isomer (−)-[^{125}I]MIBT exhibits high levels within the hippocampus, the nuclei of the fifth and seventh cranial nerves, and the cerebellum. Moderate densities are evident over the cortex and red nucleus while low levels are found within the caudate-putamen. The low density of radioactivity over the basal ganglia is inconsistent with the high levels of presynaptic cholinergic markers which have been detected within this structure.[17-19] Thus, the distribution of (−)-[^{125}I]MIBT does not reflect cholinergic innervation.

The distribution of (−)-[^{125}I]MIBT may be contrasted with that of the dextrorotary isomer, (+)-[^{125}I]MIBT

Table II. Regional Kinetics of (+)-[^{125}I]MIBT in the Rat Brain

	% dose/g of tissue (range)		
tissue	30 min	120 min	180 min
cortex	0.65	0.40	0.25
	0.59–0.68	0.34–0.47	0.22–0.30
caudate-putamen	0.64	0.67	0.49
	0.60–0.71	0.63–0.73	0.37–0.57
cerebellum	0.53	0.28	0.17
	0.43–0.64	0.21–0.36	0.14–0.19
remainder	0.59	0.40	0.25
	0.53–0.67	0.34–0.49	0.23–0.28
	Ratios		
caudate/cortex	*0.98*	*1.68*	*1.93*
caudate/cerebellum	1.20	2.43	2.95

(Figure 1b). Following intravenous injection of the latter, high densities of radioactivity are seen over the amygdala, the nucleus accumbens, the olfactory tubercle, the nuclei of the fifth and seventh cranial nerves, and the caudate-putamen. Within the latter structure, a medial-to-lateral gradient is clearly evident. A similar gradient has been reported for [^{3}H]vesamicol in the rat brain.[20] Moderate to low densities are seen over the hippocampus, cortex, and cerebellum. The regional distribution of (+)-[^{125}I]-MIBT is qualitatively similar to that reported for presynaptic cholinergic markers such as choline acetyltransferase (ChAT), acetyl cholinesterase (AChE), [^{3}H]vesamicol, and [^{3}H]hemicholinium.[17-21] The distribution of (+)-[^{125}I]MIBT therefore reflects central cholinergic innervation.

Regional Kinetics of (+)-[^{125}I]MIBT in the Rat Brain. At 30 min following the injection of the radiotracer, similar concentrations of radioactivity were observed in three major regions: striatum, cerebellum, and cortex (Table II). However, the levels in the cortex and cerebellum decreased significantly thereafter. In contrast, levels in the striatum remained fairly stable up to 120 min and decreased by only 27% between 2 and 3 h postinjection. These differential efflux rates resulted in increased striatum:cerebellum and striatum:cortex ratios at 120 and 180 min. The higher levels of radioactivity in the striatum are consistent with the high levels of cholinergic activity within this substructure. Thus the rapid efflux of radioactivity from the cortex and cerebellum probably reflects the release of the ligand from nonspecific sites.

Blocking Studies. To gain further insight into the nature of radiolabeled MIBT binding in vivo, the effect of three ligands, vesamicol, **2b**, and haloperidol, was examined. Pretreatment of animals with vesamicol reduced the brain level of (+)-[^{125}I]MIBT by 40% (Table III). Similarly, and in spite of an unexplained slight decrease in the control value, the level of (−)-[^{125}I]MIBT in the brain was decreased by 50% following vesamicol administration (Table III). The effect of vesamicol on radiotracer accumulation suggests a common binding site for vesamicol and MIBT. However, since vesamicol and some of its analogs also exhibit high affinity for σ receptors,[22] it was not clear which receptor was represented by this vesamicol-sensitive fraction. Coadministration of (+)-[^{125}I]MIBT with **2b**, a more selective vesamicol receptor ligand, reduced radiotracer levels in the striatum, cortex, and cerebellum by 58, 35, and 9%, respectively (Table IV). This observation suggests that (+)-[^{125}I]MIBT binds to the vesamicol receptor in vivo. In addition, the relative insensitivity of cerebellar levels of (+)-[^{125}I]MIBT to **2b** is consistent with the paucity of cholinergic innervation to this structure.[17,18]

Table III. Effect of Vesamicol on the Accumulation of (+)- and (−)-[^{125}I]MIBT in the Rat[a]

tissue	% dose/g of tissue (range) control	vesamicol
	(+)-[^{125}I]MIBT	
blood	0.05	0.05
	0.04–0.06	0.04–0.06
liver	2.01	1.93
	1.65–3.34	1.64–2.13
lung	1.56	1.59
	1.28–1.90	1.17–2.41
kidney	1.76	0.91
	1.55–2.08	0.83–1.11
muscle	0.16	0.13
	0.15–0.20	0.12–0.15
spleen	0.97	0.97
	0.89–1.04	0.82–1.20
heart	0.25	0.24
	0.21–0.30	0.19–0.30
brain	0.51	0.30
	0.45–0.66	0.27–0.36
gonads	0.15	0.15
	0.14–0.15	0.13–0.17
thyroid	1.77	2.02
	1.47–1.93	1.57–2.34

tissue	% dose/g of tissue (range) group 1 (n = 3)	group 2 (n = 3)
	(−)-[^{125}I]MIBT	
blood	0.11	0.12
	0.10–0.11	0.09–0.16
liver	1.91	1.89
	1.63–2.13	1.52–2.21
lung	2.36	1.59
	2.03–2.73	1.02–2.18
kidney	2.45	1.13
	1.78–2.73	0.87–1.35
muscle	0.18	0.16
	0.12–0.25	0.12–0.20
spleen	1.05	0.80
	0.92–1.18	0.62–0.94
heart	0.59	0.30
	0.57–0.61	0.22–0.35
brain	0.68	0.34
	0.67–0.69	0.27–0.38
gonads	0.15	0.16
	0.14–0.15	0.15–0.17
thyroid	2.62	4.56
	2.22–3.37	3.02–6.14
	Ratios	
brain/blood	6.45	2.75
	6.27–6.70	2.53–2.88
heart/blood	5.59	2.40
	5.27–5.81	2.32–2.56

[a] At time = 0, animals in the control group were injected intravenously with vehicle (50%) aqueous EtOH (0.2 mL), while animals in the vesamicol group received iv injections of *dl*-vesamicol (1.01 μmol/kg). After 15 min, animals in both groups were injected with the radiotracer, allowed to recover and sacrificed at 30-min postradiotracer injection.

Coadministration of (+)-[^{125}I]MIBT with haloperidol (0.5 μmol/kg), a known σ receptor ligand,[23] caused a decrease in radioactivity levels in every region studied except the striatum (Table V). In the cortex and cerebellum, haloperidol administration resulted in reductions of 34 and 60%, respectively. In contrast, the level of radioactivity in the striatum increased by 32%.

In the rat brain, σ receptor density is highest in cerebellum, pons-medulla, midbrain, red nucleus, and hippocampus.[24] Moderate densities are found in the hypothalamus and cerebral cortex, while the basal ganglia exhibit the lowest densities. The distribution of σ receptors in the rat brain is consistent with the regional effects of

Table IV. Effect of **2b** (ABV) on the Regional Distribution of (+)-[^{125}I]MIBT

region	% dose/g of tissue (range) control (n = 4)	ABV (n = 4)
cortex	0.23	0.15
	0.19–0.25	0.18–0.17
caudate-putamen	0.40	0.23
	0.35–0.47	0.21–0.26
cerebellum	0.12	0.11
	0.10–0.13	0.10–0.13
remainder	0.21	0.15
	0.17–0.23	0.14–0.17
	Ratios	
caudate/cortex	1.76	1.57
caudate/cerebellum	3.22	2.07

Table V. Effect of Haloperidol on the Regional Distribution of (+)-[^{125}I]MIBT in the Rat Brain

region	% dose/g of tissue (range) control (n = 4)	haloperidol (n = 4)
cortex	0.32	0.21
	0.29–0.38	0.15–0.25
caudate-putamen	0.75	0.99
	0.60–0.85	0.85–1.08
cerebellum	0.22	0.09
	0.18–0.24	0.09–0.09
remainder	0.33	0.17
	0.28–0.40	0.14–0.19
	Ratios	
caudate/cortex	2.32	4.82
caudate/cerebellum	3.48	10.97

haloperidol on (+)-[^{125}I]MIBT binding. However, the increased accumulation of radiotracer within the basal ganglia following haloperidol administration may be attributed to increased circulation to this structure. Similar observations have been reported for other neuroleptics.[25–27] It is also worth noting that the distribution of (−)-[^{125}I]MIBT (Figure 1a) parallels that described for the σ receptor.

In a previous structure–activity study,[28] we showed that potent vesamicol receptor ligands can be obtained from suitably substituted analogs of **1** which lack an intact cyclohexane ring. Biological evaluation of radioiodinated **13**, a representative of this class of conformationally mobile vesamicol analogs, revealed that the latter is a high-affinity ligand for both vesamicol and σ receptors.[22] The marginal selectivity of **13** for the vesamicol receptor was presumed to be largely responsible for the inability of this compound to detect reductions in cortical cholinergic innervation in the Alzheimer brain.[22] In an effort to obtain more selective ligands for this receptor, we synthesized several derivatives of 4-azavesamicol, **5**.[14] Although the latter is a poor ligand for the vesamicol receptor, many of the *N*-arylalkyl derivatives of this compound, including **6** (MIBT), were found to be potent ligands for this receptor.[14]

Although both (+)- and (−)-[^{125}I]MIBT achieve significant levels in the rat brain, the initial levels of the latter are 60% higher than those of the former. Additionally, the levels of (−)-[^{125}I]MIBT remain relatively stable over 3 h while those of (+)-[^{125}I]MIBT show a steady decline during the same period. In spite of this decline, we find that it is the distribution of (+)-[^{125}I]MIBT, not that of (−)-[^{125}I]MIBT, which reflects central cholinergic innervation. This observation is consistent with earlier reports[14] suggesting that the dextrorotatory 4-azavesamicol isomers are more potent vesamicol receptor ligands than their

corresponding antipodes. Since the central distribution of (+)-[^{125}I]MIBT at 3 h clearly reflects known cholinergic pathways, we therefore conclude that the observed efflux of (+)-[^{125}I]MIBT from the brain is largely due to the dissociation of the radiotracer from noncholinergic sites. The latter conclusion is consistent with the observation that release of radioactivity from the brain is nonuniform. Specifically, the levels of radioactivity within the cortex and cerebellum decline much faster than those in the striatum. The differential efflux of radiotracer from these regions results in a progressive increase in the striatum:cerebellum and striatum:cortex ratios over the duration of the study. Thus at 3 h postinjection, (+)-[^{125}I]MIBT presents an image which is strikingly different from that obtained with the static (−)-[^{125}I]MIBT.

Although (+)- and (−)-[^{125}I]MIBT reveal different distribution patterns in the brain at 3 h postinjection, the accumulation of both compounds is reduced by the *dl*-vesamicol. Since the levels of (−)-MIBT remain stable throughout the duration of the study, while the distribution of this radiotracer fails to reflect cholinergic innervation, we conclude that the vesamicol-sensitive component of (+)- and (−)-[^{125}I]MIBT binding represents a fraction bound to noncholinergic sites. In this connection, we note that vesamicol is a marginally selective ligand with high affinity for both σ and vesamicol receptors (vide supra). The marginal selectivity of vesamicol suggests that this ligand is poorly suited for in vivo blocking studies with potential vesamicol receptor ligands. This view is supported by an earlier report[7] suggesting that the central distribution of [^{3}H]vesamicol in vivo is inconsistent with that of known presynaptic cholinergic markers.

Choline acetyltransferase (ChAT) and acetylcholinesterase (AChE), enzymes which respectively synthesize and degrade acetylcholine, are recognized as two of the most prominent markers of cholinergic innervation.[29] Consequently, the distribution of these enzymes in the brain provides a benchmark against which related cholinergic markers may be evaluated. Previous studies[17] have shown that the levels of ChAT in the striatum are 25 and 10 times higher than those in the cerebellum and cortex, respectively. The corresponding values for AChE are 7 and 2, respectively. In spite of the obvious qualitative similarities between the distribution of (+)-[^{125}I]MIBT and these cholinergic markers, quantitative discrepancies are easily discernible. Specifically, the striatum:cerebellum and striatum:cortex ratios for (+)-[^{125}I]MIBT are significantly lower than those reported for either ChAT or AChE. However, these ratios were increased substantially by coadministration of the radiotracer with haloperidol, suggesting that (+)-[^{125}I]MIBT binds to both vesamicol and σ receptors in vivo. Further evidence of σ receptor involvement is provided by the observation that haloperidol differentially affects the regional kinetics of (+)-[^{125}I]MIBT, decreasing the levels of radiotracer in the cortex and cerebellum while increasing radiotracer levels in the striatum. Additionally, the percent reduction in radiotracer levels is greater in the cerebellum (59%) than the cortex (34%). Thus, the rank order of the effect of haloperidol on the regional accumulation of (+)-[^{125}I]-MIBT is as follows: cerebellum > cortex ≫ striatum. Interestingly, this rank order parallels the regional densities of σ receptors in the rat brain,[24] thereby providing additional support for the role of these receptors in determining the kinetics of (+)-[^{125}I]MIBT in vivo. However, further investigation may be needed to better define the effect of regional σ receptor density on the distribution of (+)-[^{125}I]MIBT.

Finally, the introduction of a nitrogen atom into the cyclohexyl moiety of vesamicol provides opportunities for the development of novel radioligands for the vesamicol receptor. The central distribution of (+)-[^{125}I]MIBT, one compound from this class of vesamicol receptor ligands, is consistent with the distribution of central cholinergic pathways. Thus (+)-[^{123}I]MIBT may be potentially useful for mapping cholinergic innervation in vivo. However, the slow dissociation of this radiotracer from σ receptor sites may require that radiotracer administration precede SPECT imaging by several hours. Alternatively, clearance of radiotracer from σ receptor sites may be facilitated by preadministration of haloperidol.

Experimental Section

General. Synthetic intermediates were purchased from Aldrich, Inc. (Milwaukee, WI) and were used as received. Solvents were distilled immediately prior to use. Commercially available reagents were used without further purification. Tissue Tek OCT compound was purchased from Miles Inc., Elkhart, IN. Rats and mice were obtained from Sasco Inc., Omaha, NE.

Reactions involving air-sensitive reagents were carried out under nitrogen. Melting points were determined on a Mel-Temp melting point apparatus and are uncorrected. The specific rotation was determined on an automatic polarimeter (Autopol III, Rudolph Research, Flanders, NJ). ^{1}H NMR spectra were recorded on an IBM-Brucker spectrometer at 200 MHz. NMR spectra are referenced to the deuterium lock frequency of the spectrometer. Under these conditions, the chemical shifts (in ppm) of residual solvent in the ^{1}H NMR spectra were found to be as follows: $CHCl_3$, 7.26; DMSO, 2.56; HOD, 4.81. The following abbreviations are used to describe peak patterns whenever appropriate: br = broad, s = singlet, d = doublet, t = triplet, q = quartet, m = multiplet. Low- and high-resolution mass spectrometry was performed on an AEI MS-30 instrument. Elemental analyses were performed by Atlantic Microlab, Inc., Norcross, GA. Unless otherwise indicated, these values are within ±0.4% of the theoretical.

Column chromatography was performed using "Baker analyzed" silica gel (60–200 mesh). Preparative chromatography was performed on either a Harrison Research Chromatotron using Merck 60 PF_{254} silica gel or by HPLC (Rainin Instrument Co.) using a 41.1-mm-i.d. Dynamax silica gel column (at a solvent delivery rate of 80 mL/min). Enantiomeric purity was determined by HPLC with a 25-cm × 4.6-mm-i.d. Chiralcel OD column (isopropropyl alcohol, 10:hexane, 89:Et_3N, 1; flow rate 1 mL/min). Analytical TLC was performed on Analtech glass TLC plates coated with silica gel GHLF and were visualized with UV light and/or methanolic iodine. All target compounds were checked for purity by HPLC (silica gel, 10–20% isopropyl alcohol–hexanes, 1% Et_3N).

1-(3-(Tri-*n*-butylstannyl)benzyl)-4-hydroxy-3-(4-phenylpiperidinyl)piperidine (8). A solution of *n*-BuLi (4.0 mmol) in hexanes (1.6 mL) was added dropwise under N_2 to a stirring solution of 7 (0.77 g, 1.8 mmol) in dry THF (10 mL) cooled to −70 °C (dry ice–acetone). After the mixture was stirred at −70 °C for 135 min, a solution of *n*-Bu_3SnCl (0.65 g, 2.0 mmol) in dry THF (8 mL) was added over 10 min. The dry ice–acetone bath was removed, and the mixture was allowed to warm up to room temperature. After 20 h, the reaction was quenched with 5% aqueous NH_4Cl (25 mL), and the mixture was extracted with CH_2Cl_2 (3 × 25 mL). The combined organic extracts were dried over anhydrous Na_2SO_4 and concentrated to an oil. The crude product was purified by radial flow chromatography on silica gel (acetone, 25:hexanes, 75:Et_3N, 1) to yield 0.31 g (27%) of a pale yellow syrup: ^{1}H NMR ($CDCl_3$) δ 1.59–2.07 (m, 38H), 2.27 (t, 1H), 2.48–2.60 (m, 2H), 2.76 (t, 1H), 2.94 (d, 2H), 3.05 (d, 2H), 3.44–3.61 (m, 1H), 7.20–734 (m, 9H); CIMS *m/e* (intensity) 639.0 ($M^+ + H^+$, 1.78), 640.9 ($M^+ + H^+$, 2.43).

3-(Tri-*n*-butylstannyl)benzyl Alcohol (10). A solution of 2.5 M *n*-BuLi in hexane (4.7 mL) was added dropwise under N_2 to a cooled (−78 °C) stirring solution of 3-bromobenzyl alcohol, **9** (1.0 g, 5.3 mmol), in dry THF (25 mL). The resulting mixture was stirred at −78 °C for 90 min. At this time, a solution of *n*-Bu_3SnCl (3.82 g, 11.74 mmol) in dry THF (10 mL) was added dropwise. Following the addition, the dry ice–acetone bath was removed and stirring was continued for 20 h. The reaction was quenched with 5% aqueous NH_4Cl (40 mL), and the mixture was extracted with CH_2Cl_2 (3 × 50 mL). The combined organics were dried over anhydrous Na_2SO_4 and concentrated to a pale yellow liquid. The latter was purified by radial flow chromatography on silica gel (hexanes, 90:acetone, 10:Et_3N, 1) to yield 1.5 g (71%) of the product as a colorless liquid: ^1H NMR ($CDCl_3$) δ 0.89 (t, 9H), 1.10 (t, 6H), 1.35 (m, 6H) 1.49 (m, 6H), 4.68 (s, 1H), 7.36 (m, 4H); CIMS *m/e* (intensity) 640.9 (M^+ + 2, 1.78). Anal. ($C_{19}H_{34}OSn$) C, H.

(+)- and (−)-4-Hydroxy-1-(3-iodobenzyl)-3-(4-phenylpiperidinyl)piperidine [(+)-6 and (−)-6].[14] The synthesis of racemic **6** has been described. This compound was resolved chromatographically on a 10-mm-i.d. Chiralcel OD column (i-PrOH, 10:hexane, 89:Et_3N, 1) to yield pure (+)-**6**, $[\alpha]_D$ = +9.6 (*c* = 0.016 g/mL, MeOH), and (−)-**6**. At a flow rate of 5 mL/min, the retention times of (+)- and (−)-**6** were 9.5 and 12.7 min, respectively.

Radiolabeling. Method 1: (+)- and (−)-4-Hydroxy-1-(3-[^{125}I]iodobenzyl)-3-(4-phenylpiperidinyl)piperidine [(+)-[^{125}I]-6 and (−)-[^{125}I]-6]. Five microliters of a stock solution of **8** (13.4 mM in EtOH) was added to a 10- × 75-m borosilicate tube capped with a rubber septum and vented with a charcoal filter. To this solution were added EtOH (50 μL), glacial HOAc (50 μL), an aqueous solution of 970 μCi of $Na^{125}I$ in NaOH (pH 10), and Chloramine T (5 mg). The vial was vortexed for 15 s and allowed to stand at room temperature. After 15 min, the reaction was quenched with 5% aqueous $NaHSO_3$ (100 μL). The mixture was subsequently neutralized with saturated Na_2CO_3 (300 μL) and extracted with CH_2Cl_2 (3 × 0.5 mL). The combined organic extracts were dried over anhydrous Na_2SO_4, diluted with a solution of 40% oxalic acid in EtOH (50 μL), and concentrated under a stream of N_2. The residue which contained 730 μCi was redissolved in 50% i-PrOH–hexane (100 μL) and purified by HPLC on a 25-cm × 4.6-mm-i.d. Chiralcel OD column (i-PrOH,10: hexane, 89:Et_3N, 1; flow rate 1 mL/min) to provide 238 μCi (24% radiochemical yield) of (+)-[^{125}I]-**6** and 178 μCi (18.4% radiochemical yield) of (−)-[^{125}I]-**6**. The radiochemical purities of (+)-[^{125}I]-**6** and (−)-[^{125}I]-**6** were 95.7% and 98.8%, respectively. Under the conditions used for chromatography, the retention times of the dextrotatory and levorotatory enantiomers were found to be 8.5 and 12.7 min, respectively. Their respective enantiomeric purities were greater than 98%.

Method 2. Stock solutions of the following reagents were prepared for radiolabeling: Chloramine T (20 mg/mL in H_2O), (+)-trozamicol (2 mg/mL in CH_3CN, 98:Et_3N, 2), oxalic acid (40 mg/mL in MeOH), and **10** (10.6 mM in MeOH). To a borosilicate tube equipped with a rubber septum and vented with a column of charcoal were added the reagents in the following order: **10** (50 μL, 500 nmol), glacial HOAc (50 μL), aqueous $Na^{125}I$ (1.90 mCi, pH 8–10), and Chloramine T (30 μL). The resulting solution was vortexed for 30 s and allowed to stand for 30 min. The reaction was quenched with 5% aqueous $NaHSO_3$ (100 μL) and saturated $NaHCO_3$ (500 μL) and vortexed for 30 s. The resulting mixture was extracted with CH_2Cl_2 (3 × 1 mL). The combined organic extracts were passed through a short column of anhydrous Na_2SO_4 and collected in a second borosilicate tube. The extract was concentrated under a stream of nitrogen to provide a residue.

The latter was treated with 48% HBr (1 mL), and the solution was heated at 90 °C for 30 min. The mixture was cooled to room temperature and extracted with CH_2Cl_2 (3 × 1 mL). The organic extracts were first passed through a short column of anhydrous sodium sulfate and then through a short column of anhydrous sodium carbonate. The eluent was collected in a third borosilicate tube. This solution was treated with (+)-trozamicol (100 μL, 0.6 μmol) and subsequently concentrated under a stream of nitrogen to yield 1.59 mCi of the crude intermediate. The concentrate was redissolved in DMF (50 μL) and Et_3N (30 μL) and heated at 110 °C for 30 min. After the first 15 min, more Et_3N (20 μL) was added down the sides of the reaction vessel to wash down unreacted material. Finally, the reaction mixture was cooled to room temperature and diluted with absolute EtOH (50 μL).

Upon radioassay, the reaction mixture was found to contain 1.57 mCi (83% recovery). Analysis by HPLC (Dynamax C_{18} reverse-phase column) revealed that the reaction mixture contained (+)-[^{125}I]MIBT in 91% radiochemical purity. The product was purified by C_{18} reverse-phase HPLC (90% MeOH–5 mM phosphate buffer, pH 7.8) to yield 0.74 mCi (39% radiochemical yield) of (+)-[^{125}I]MIBT. From a standard curve (Beer–Lambert), the specific activity of the product was estimated to be 150–200 Ci/mmol.

Biological. Tissue Distribution Experiments. Four groups of male Wistar rats (*n* = 4) weighing 200–350 g were used in these experiments. Each animal received, while under ether anesthesia, an intravenous injection of the radiotracer (3–5 μCi) dissolved in 0.1 mL of 50% aqueous ethanol. At 5, 30, 60, and 180 min postinjection, blood was collected from the anesthetized animal by cardiac puncture, and the animal was immediately sacrificed by cardiectomy. The organs and tissues of interest were harvested and transferred to preweighed tubes, and the radioactivity was measured with a Beckman γ counter. The tubes were subsequently reweighed to give the weights of the corresponding tissues. Preweighed tubes containing 1-mL samples of a 1:100 dilution of the injected dose were also counted and used as reference for calculating the fractional tissue levels of radioactivity. The accumulation of radiotracer was expressed as a percentage of the injected dose per gram of tissue.

Regional Kinetics of (+)-[^{125}I]MIBT in the Rat Brain. Three groups of male Wistar rats (*n* = 4) were used for this experiment. While under ether anesthesia each animal received an intravenous injection of (+)-[^{125}I]MIBT (2 μCi in 100 μL of 50% aqueous EtOH). The animals were subsequently sacrificed at 30, 120, and 180 min postinjection. The brains were harvested, partially frozen, and dissected into three main regions: striatum, cerebellum, and cortex. The radioactivity in these three regions and the remainder of the brain was measured with a Beckman γ camera. The fractional tissue activity was calculated as described above.

Blocking Studies. Experiment 1. Animals in group 1 (*n* = 4) each received an intravenous injection of the radiotracer (3 μCi in 100 μL of 50% aqueous EtOH). Animals in group 2 (*n* = 4) were injected iv with a similar dose of the radiotracer mixed with **2b** (0.1 μmol/kg). At 180 min postinjection, the animals were sacrificed, and the tissues were harvested as outlined above.

Experiment 2. Animals in group 1 (*n* = 4) were injected intravenously with 100 μL of 50% aqueous EtOH (vehicle). The animals in group 2 (*n* = 4) received, at the same time, iv injections of *dl*-vesamicol (1.01 μmol/kg) in 50% aqueous EtOH. After 15 min, animals in both groups were injected intravenously with the radiotracer (2.0 μCi in 100 μL of 50% aqueous EtOH). All animals were sacrificed 30 min following radiotracer administration. Tissues were harvested as described above, and the data was analyzed in a similar manner.

Experiment 3. Animals in the control groups (*n* = 4) received iv injections of (+)-[^{125}I]MIBT only (1 μCi in 100 μL of 50% aqueous EtOH). In the second group (*n* = 4), each animal received an iv injection of (+)-[^{125}I]MIBT (1 μCi) and haloperidol oxalate (0.5 μmol/kg) in 100 μL of the same solvent. All animals were sacrificed after 3 h. The brains were removed, partially frozen, and dissected into three major brain regions: striatum, cerebellum, and cortex. The fractional accumulation of radioactivity within these regions and the rest of the brain was calculated, using suitable dilutions of the injected dose, as described above.

Ex Vivo Autoradiographic Studies. Two groups of male Wistar rats (*n* = 2) were used in these experiments. Each animal in the first group received an intravenous injection of (+)-[^{125}I]MIBT (385 μCi in 0.1 mL of 50% aqueous EtOH). Similarly, animals in the second group received 330 μCi of (−)-[^{125}I]MIBT (in 0.1 mL of 50% aqueous EtOH). After 3 h, the animals were sacrificed by decapitation. The brains were carefully removed, embedded in Tissue Tek OCT medium, and frozen to −37 °C. Twenty-micron coronal brain slices were subsequently obtained by sectioning rostrocaudally with a Reichert HistoSTAT microtome at −15 °C. The tissue sections were apposed to Kodak NMC film accompanied by ^{125}I-labeled external standards (^{125}I-

Microscales from Amersham). For delineation of cytoarchitecture, adjacent tissue sections were subjected to Nissl staining.

Acknowledgment. Financial support was provided by the NINDS (Grant #NS28711) and Alzheimer's Disease Research, a program of the American Health Assistance Foundation. The authors express their gratitude to Ms. Charla Zaccardi for the preparation of this manuscript.

References

(1) Bahr, B. A.; Parsons, S. M. Demonstration of a receptor in *Torpedo* synaptic vesicles for the acetylcholine storage blocker L-trans-2-(4-phenyl[3,4-^{3}H]piperidino)cyclohexanol. *Proc. Natl. Acad. Sci. U.S.A.* **1986**, *83*, 2267–2270.

(2) Marshall, I. G.; Parsons, S. M. The vesicular acetylcholine transport system. *Trends Neurol. Sci.* **1987**, *10*, 174–177.

(3) Marshall, I. G. Studies on the blocking action of 2-(4-phenylpiperidino)cyclohexanol (AH5183). *Br. J. Pharmacol.* **1970**, *38*, 503–516.

(4) Wannan, G.; Prior, C.; Marshall, I. G. α-Adrenoceptor blocking properties of vesamicol. *Eur. J. Pharmacol.* **1991**, *201*, 29–34.

(5) Rogers, G. A.; Parsons, S. M.; Anderson, D. C., Nilsson, L. M.; Bahr, B. A.; Kornreich, W. D.; Kaufman, R.; Jacobs, R. S.; Kirtman, B. Synthesis, in vitro acetylcholine-storage-blocking activities, and biological properties of derivatives and analogues of trans-2-(4-phenylpiperidino)cyclohexanol (vesamicol). *J. Med. Chem.* **1989**, *32*, 1217–1230.

(6) Rogers, G. A.; Parsons, S. M. Persistent occultation of the vesamicol receptor. *NeuroReport* **1990**, *1*, 22–25.

(7) Jung, Y.-W.; Van Dort, M. E.; Gildersleeve, D. L.; Wieland, D. M. A radiotracer for mapping cholinergic neurons of the brain. *J. Med. Chem.* **1990**, *33*, 2065–2068.

(8) Kilbourn, M. R.; Jung, Y.-W.; Haka, M. S.; Gildersleeve, D. L.; Kuhl, D. E.; Wieland, D. M. Mouse brain distribution of a carbon-11 labelled vesamicol derivative: presynaptic marker of cholinergic neurons. *Life Sci.* **1990**, *47*, 1955–1963.

(9) Efange, S. M. N.; Dutta, A. K.; Michelson, R. H.; Kung, H. F.; Thomas, J. R.; Billings, J.; Boudreau, R. J. Radioiodinated 2-hydroxy-3-(4-iodophenyl)-1-(4-phenylpiperidinyl)propane: potential radiotracer for mapping central cholinergic innervation in vivo. *Nucl. Med. Biol.* **1992**, *19*, 337–348.

(10) Widen, L.; Eriksson, L.; Ingvar, M.; Parsons, S. M.; Rogers, G. A.; Stone-Elander, S. Positron emission tomographic studies of central cholinergic nerve terminals. *Neurosci. Lett.* **1992**, *136*, 1–4.

(11) Mulholland, G. K.; Jung, Y.-W.; Sherman, P. S.; Pisani, T. L.; Kuhl, D. E.; Wieland, D. M.; Kilbourn, M. R. Efficient one-step synthesis of (−)-[^{18}F]fluoroethoxy-benzovesamicol (FEOBV): A new tracer for mapping cholinergic neurons in vivo. *Abstr. IXth Intl. Symposium on Radiopharmaceutical Chem.* **1992**, 487–488.

(12) Mulholland, G. K.; Buck, F.; Sherman, P. S.; Pisani, T. L.; Jung, Y.-W.; Frey, K. A.; Kuhl, D. E.; Kilbourn, M. R. 4-[^{18}F]Fluorobenzyl-ABV: a new potential marker for central cholinergic presynaptic sites. *J. Nucl. Med. (Suppl.)* **1991**, *32*, 994.

(13) Rogers, G.; Stone-Elander, S.; Eriksson, L.; Ingvar, M.; Parsons, S.; Widen, L. [^{18}F]Vesamicol derivatives for in vivo evaluation as tracers for cholinergic synaptic vesicles. *IXth International Symposium on Radiopharmaceutical Chemistry* **1992**, 486.

(14) Efange, S. M. N.; Khare, A. B.; Parsons, S. M.; Bau, R.; Metzenthin, T. Non-symmetrical bipiperidyls as inhibitors of vesicular acetylcholine storage. *J. Med. Chem.*, in press.

(15) Zalutsky, M. R.; Narula, A. S. A method for the radiohalogenation of proteins resulting in decreased thyroid uptake of radioiodine. *Appl. Rad. Isot.* **1987**, *38*, 1051–1055.

(16) Moerlein, S. M.; Coenen, H. H. Regiospecific no-carrier-added radiobromination and radioiodination of aryltrimethyl group 1Vb organometallics. *J. Chem. Soc., Perkin Trans. 1* **1985**, 1941–1947.

(17) Stavinoha, W. B.; Weintraub, S. T.; Modak, A. T. Regional concentrations of choline and acetylcholine in the rat brain. *J. Neurochem.* **1974**, *23*, 885–886.

(18) Kuczenski, R.; Segal, D. S.; Mandell, A. J. Regional and subcellular distribution and kinetic properties of rat brain choline acetyltransferase - some functional considerations. *J. Neurochem.* **1975**, *24*, 39–45.

(19) Quirion, R. Characterization and autoradiographic distribution of hemicholinium-3 high-affinity choline uptake sites in mammalian brain. *Synapse* **1987**, *1*, 293–303.

(20) Marien, M. R.; Parsons, S. M.; Altar, C. A. Quantitative autoradiography of brain binding sites for the vesicular acetylcholine transport blocker 2-(4-phenylpiperidino)cyclohexanol (AH5183). *Proc. Natl. Acad. Sci. U.S.A.* **1987**, *84*, 876–880.

(21) Altar, C. A.; Marien, M. R. [^{3}H]vesamicol binding in brain: Autoradiographic distribution, pharmacology, and effects of cholinergic lesions. *Synapse* **1988**, *2*, 486–493.

(22) Efange, S. M. N.; Mash, D. C.; Basile, M.; Pablo, J.; Kung, H. F.; Michelson, R. H.; Thomas, J. R. The vesamicol receptor (VR): Radioligand selectivity and the detection of central cholinergic hypofunction. *Abstr. IXth Intl. Symposium on Radiopharmaceutical Chem.* **1992**, 311–312.

(23) Largent, B. L.; Wilkstrom, H.; Gundlach, A. L.; Snyder, S. H. Structural determinants of sigma receptor affinity. *Mol. Pharmacol.* **1987**, *32*, 772–784.

(24) Gundlach, A. L.; Largent, B. L.; Snyder, S. H. Autoradiographic localization of sigma receptor binding sites in guinea pig and rat central nervous system with (+)-^{3}H-3-(3-hydroxyphenyl)-N-(1-propyl)-piperidine. *J. Neurosci.* **1986**, *6*, 1757–1770.

(25) Weissman, A. D.; Broussolle, E. P.; London, E. D. In vivo binding of [^{3}H]d-N-allylnormetazocine and [^{3}H]haloperidol to sigma receptors in the mouse brain. *J. Chem. Neuroanat.* **1990**, *3*, 347–354.

(26) Barone, D.; Luzzani, F.; Assandri, A.; Galliani, G.; Mennini, T.; Garattini, S. In vivo stereospecific [^{3}H]spiperone binding in rat brain: characteristics, regional distribution, kinetics and pharmacological properties. *Eur. J. Pharmacol.* **1985**, 63–74.

(27) Goeders, N. E.; Ritz, M. C.; Kuhar, M. J. Buspirone enhances benzodiazepine receptor binding in vivo. *Neuropharmacology* **1988**, *27*, 275–280.

(28) Efange, S. M. N.; Michelson, R. H.; Dutta, A. K.; Parsons, S. M. Acyclic analogues of 2-(4-phenylpiperidino)cyclohexanol (vesamicol): conformationally mobile inhibitors of vesicular acetylcholine transport. *J. Med. Chem.* **1991**, *34*, 2638–2643.

(29) Satoh, K.; Armstrong, D. M.; Fibiger, H. C. A comparison of the distribution of central cholinergic neurons as demonstrated by acetylcholinesterase pharmacohistochemistry and choline acetyltransferase immunohistochemistry. *Brain Res. Bull.* **1983**, *11*, 693–720.